# Formation of a quasistationary state by Gaussian wave packet scattering on a lattice of *N* identical delta potentials

Yu. G. Peisakhovich and A. A. Shtygashev

*Novosibirsk State Technical University, Novosibirsk, Russia*

It is considered a Gaussian quantum wave packet scattering on the finite periodic lattice composed of *N* identical $\delta$ barriers or $\delta$ wells. The parameters of general theory are expressible through the characteristics of wave packet and lattice. We explain the results of numerical simulation for the processes in the lattice of *N* =50 $\delta$ barriers. The directly measurable in the experiments probability of the particle finding in lattice, the local probability density, and the probability current are founded.

PACS number(s): 73.21.Cd, 03.65.−w, 73.40.Gk

## I. INTRODUCTION

In our previous paper[1] we have studied theoretically the possibility of formation and further evolution of specific quasistationary states accompanying the scattering of quantum wave packets in the one-dimensional finite periodic structures. The effect should be mostly noticeable for the lengthy wave packet with the narrow spectral function covering one or a few lines of the total transparency near thresholds of the lattice transmission band. The tight binding lattice potential is preferable but its shape in the unit cell may be arbitrary to a considerable degree.

In this paper we consider a model describing the scattering of the initially Gaussian wave packet on the finite periodic lattice composed of *N* identical $\delta$ barriers or $\delta$ wells. The parameters of general theory are expressible now through the characteristics of wave packet and lattice. Moreover, we explain the results of numerical modeling for mentioned processes in the lattice consisting of the *N*=50 identical $\delta$ barriers.

The $\delta$-comb limit of the Kronig-Penny type models simplifies our analysis and calculations of the physical processes because we can neglect the shape and width of the lattice barriers and concentrate our attention on the trigonometric factors depending of the period *d* of the system. Together with the power of $\delta$ potentials it gives the main information about the resonances of scattering in the lattice.[2] Moreover, this model describes real superlattices composed of very thin atomic $\delta$ layers.[3]

The consideration of wave packet scattering on the system composed of two or more $\delta$ barriers is useful for the modeling of the resonant tunnel diodes[4,5] and cascade lasers[6] in certain regimes. The scattering of wave packet by two $\delta$ barriers was repeatedly discussed earlier, for example in the works.[7–10] The stages of exponential and nonexponential decaying were studied there especially for the initial state $\Psi(x,0)$ localized between or near the $\delta$ barriers.[8–11] In these works, the results are characterized by the only time dependent survival probability for the particle in subsequent nonstationary state $\Psi(x,t)$ defined as

$$W(t) = \left| \int_{-\infty}^{\infty} \Psi^*(x,0)\Psi(x,t)dx \right|^2.$$

In contrast, we describe practically all stages of the concrete physical process that includes the forming and decay of the

quasistationary states in the one-dimensional finite periodic lattice at the quantum wave packet scattering on this lattice. In our discussion we operate in terms of the values that are directly measurable in the experiments by the scattering of wave packet in nanocrystals and superlattices—the probability of the particle finding in lattice $w_L=w_L(t)$, the local probability density $|\Psi(x,t)|^2$, and the probability current $j_w(x,t)$. The energy is measured in electron volts (eV), the length in angstroms (Å), but for some of the physical values we use the atomic units denoted as a.u.

## II. SETTING OF PROBLEM

Let us consider the one-dimensional lattice consisting of *N* identical $\delta$ barriers or $\delta$ wells of power $\Omega$ disposed on the distance *d* from each other (Fig. 1) and forming the potential

$$U(x) = \frac{\hbar^2}{2m}\Omega\sum_{n=1}^{N} \delta(x - nd), \qquad (2.1)$$

the parameter $\Omega$ is a positive value for the $\delta$ barriers and negative for the $\delta$ wells, i.e., the main considered effects are valid for the scattering below and above barriers, and at *t* =0 on the left of the lattice the Gaussian wave packet is formed

$$\Psi(x,0) = \frac{1}{\sqrt{\Delta x \sqrt{\pi}}} \exp\left( ik_C x - \frac{(x - x_C)^2}{2(\Delta x)^2} \right), \qquad (2.2)$$

with it's width $\Delta x$ and main wave number $k_C$ whose center is
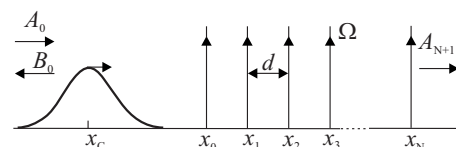


FIG. 1. Wave packet falling on the lattice of $\delta$ barriers.

localized at $x=x_C<0$ and moves to the right with the group velocity $v_C=\hbar k_C/m$ of free moving.

The spectral function $c(E)$ of the packet is determined by the stationary at energy $E$ wave functions $\psi(E,x)$ as the in-

tegral [Ref. 1, (2.2)] and when the conditions $k_C^{-1}\ll\Delta x\ll|x_C|\ll k_C(\Delta x)^2$ are fulfilled $c(E)$ is approximately equal to the expression for the free Gaussian wave packet

$$c(E) = \begin{cases} \dfrac{1}{\hbar}\sqrt{\dfrac{m\Delta x}{\sqrt{\pi}k}}\exp\left(-\dfrac{(\Delta x)^2}{2}(k-k_C)^2\right)\exp[ix_C(k_C-k)], & E\geq 0, \\ 0, & E<0. \end{cases} \tag{2.3}$$

where $k=\hbar^{-1}\sqrt{2mE}$.

## III. STATIONARY SCATTERING

The base wave functions of the stationary scattering with the energy $E>0$ are normalized on the $\delta$ function of energy and take a form

$$\psi(E,x) = \begin{cases} A_0\exp(ikx) + B_0\exp(-ikx), & x<0, \\ \psi_{0N}(E,x), & 0<x<Nd, \\ A_{N+1}\exp[ik(x-Nd)], & x>Nd, \end{cases} \tag{3.1a}$$

here $A_0=\hbar^{-1}\sqrt{m/2\pi k}$, $B_0=r(k)A_0$, and $A_{N+1}=t(k)A_0$ are partial amplitudes of the falling, reflected, and transmitted waves; $r(k)$ and $t(k)$ are reflection and transmission amplitudes.

The matrix of transfer through the cell of periodicity for the considered structure is equal to

$$M = M_\Omega M(d), \quad M_\Omega = \begin{pmatrix} 1 & 0 \\ \Omega & 1 \end{pmatrix},$$

$$M(d) = \begin{pmatrix} \cos kd & \dfrac{\sin kd}{k} \\ -k\sin kd & \cos kd \end{pmatrix}, \tag{3.1b}$$

where $M_\Omega$ is the matrix of transfer through $\delta$ potentials and $M(d)$ through the intervals between them. The wave function $\psi=\psi_{0N}(E,x)$ inside the $n$th cell has [according to Ref 1, (3.7), since in this case $M_x=M(x)$] the following form:

$$\psi_{0N}(E,x) = A_n e^{ik[x-(n-1)d]} + B_n e^{-ik[x-(n-1)d]},$$

$$(n-1)d\leq x\leq nd,$$

and the partial amplitudes in $n$th cell are expressed via partial amplitudes of falling $A_0$ and reflected $B_0$ waves by means of

$$\begin{pmatrix} A_{n+1} \\ B_{n+1} \end{pmatrix} = M_{nef}\begin{pmatrix} A_0 \\ B_0 \end{pmatrix}, \quad M_{nef}=L^{-1}M^n L. \tag{3.2}$$

Then it is valid that the expression for the values in nodes

$$\psi_{0N}(E,x_0+nd) = A_{n+1} + B_{n+1} = A_0[\psi(n) + r\psi^*(n)], \tag{3.3}$$

in which

$$\psi(n) = (M_{nef})_{22}^* + (M_{nef})_{21} \tag{3.4}$$

and coming from the reality $M$ analogical [Ref. 1, (3.11)] relations between the elements of the effective transfer matrix: $(M_{nef})_{11}=(M_{nef})_{22}^*$ and $(M_{nef})_{12}=(M_{nef})_{21}^*$ were used. We express the needed elements of the effective transfer matrix from the Abele formula [Ref. 1, (3.2)], and Eqs. (3.1b) and (3.2),

$$(M_{nef})_{22} = U_{n-1}(y)\left(1+i\frac{\Omega}{2k}\right)e^{-ikd} - U_{n-2}(y), \tag{3.5}$$

$$(M_{nef})_{21} = iU_{n-1}(y)\frac{\Omega}{2k}e^{ikd}, \tag{3.6}$$

where $U_{n-1}(y)$ are the Chebyshev polynomials of the second kind, their argument $y$ is equal to the Kronig-Penny function now

$$y = \frac{1}{2}\mathrm{Sp}M = \cos kd + \frac{\Omega}{2k}\sin kd.$$

Hence the function (3.4) has a form

$$\psi(n) = U_{n-1}(y)e^{ikd} - U_{n-2}(y). \tag{3.7}$$

After substituting Eq. (3.7) into Eq. (3.3) we get the expression [Ref. 1, (3.8)] for the envelope

$$\psi_{0N}(E,x_0+nd)$$
$$= \begin{cases} \alpha_+\exp(iKnd) + \alpha_-\exp(-iKnd), & |y|<1, \\ \tilde\alpha_+\exp(\tilde Knd) + \tilde\alpha_-\exp(-\tilde Knd), & |y|>1, \end{cases}$$

with the effective partial amplitudes equal to

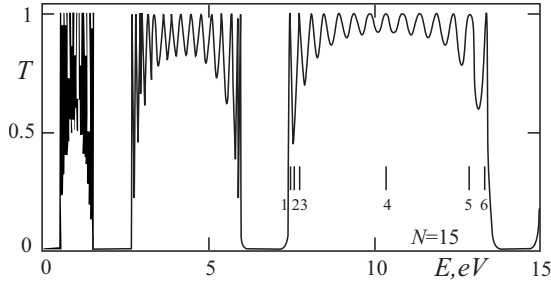$$\alpha_\pm = \mp\frac{iA_0}{2\sin Kd}[(e^{ikd}-e^{\mp iKd}) + r(e^{-ikd}-e^{\mp iKd})],$$

FIG. 2. Transmission coefficient spectrum $T = T(E)$ for the states of stationary scattering by the lattice of $N = 15$ identical $\delta$ barriers of the power $\Omega = 0.5$ a.u. disposed on the distance $d = 5$ Å from each other.

$$\tilde{\alpha}_{\pm} = \pm \frac{A_0(\operatorname{sgn} y)^n}{2 \operatorname{sh} \tilde{K} d} [(e^{kd} - (\operatorname{sgn} y) e^{\mp \tilde{K} d})$$
$$+ r(e^{-kd} - (\operatorname{sgn} y) e^{\mp \tilde{K} d})]. \tag{3.8}$$

Figures 2 and 3 illustrate behavior of the transmission coefficient $T = |t(k)|^2 = T(E)$ and the shape of the typical wave functions of stationary scattering in the $\delta$ lattice.

The spectrum $T(E)$ is composed of alternate transmission and attenuation bands and corresponds to the qualitative analysis developed in Ref. 1. The wave functions in their structure show the peculiarities of the amplitude modulated Bloch wave functions and of the wave functions of the resonant stationary scattering on a single potential barrier or well with its length equal to the lattice length.
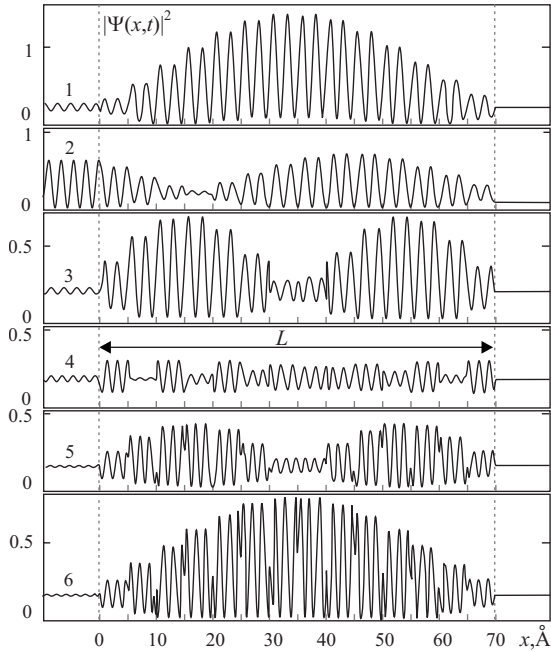


FIG. 3. Probability density for the states of stationary scattering on the lattice of $N = 15$ identical $\delta$ barriers corresponding to the spectral points were numerated in Fig. 2: (1), (3), (5), (6) near the resonance lines of total transparency, (2) between the lines, and (4) in the middle of transmission band.

## IV. ZEROS AND POLES OF THE REFLECTION AMPLITUDE

Zeros of the reflection amplitude $r(k)$ give the energies of full resonant transparency at the stationary scattering. Poles of $r(k)$ give the energies and lifetimes of quasistationary states. The dependence of these parameters from the quantity $N$ of the lattice cells was found in Ref. 1 for the arbitrary lattice potential providing the tight binding. The results include the values of three functions $\bar{y}(k_0)$, $\bar{\bar{y}}(k_0)$, and $y(k_0) = (-1)^S$ defined by the formula in Ref. 1, (3.13), as well as $y'(k_0) = dy(k_0)/dk$, are determined in some threshold point $k = k_0 \approx s\pi/d$.

For the considered model of the $\delta$ lattice from Ref. 1, (3.13) and the expression (3.1b) of the transfer matrix across the cell $M$ we get

$$\bar{y} = -i\left(\sin kd - \frac{\Omega}{2k} \cos kd\right), \quad \bar{\bar{y}} = i\frac{\Omega}{2k} \exp ikd.$$
$$\tag{4.1a}$$

The condition of tight binding $|\Omega/k| \approx |\Omega d/s\pi| \gg 1$ in $s$th transmission band $|y| < 1$ gives the dependence

$$E \approx E_S(k_0) + (-1)^S \Delta E_S \cos Kd. \tag{4.1b}$$

Here

$$E_S(k_0) = E_{S0} - \Delta E_S, \quad E_{S0} = \frac{\hbar^2 \pi^2 s^2}{2md^2}, \quad \Delta E_S = \frac{4}{\Omega d} E_{S0}.$$

The values of $k_0 = s\pi/d$ and $y = (-1)^S$, $\bar{y}(k_0) = \bar{\bar{y}}(k_0) = i(-1)^S \Omega d/2s\pi$ correspond to the top of the $s$th transmission band. Moreover, the inequalities are satisfied in this band $|\Delta k_1|, |k_2| \ll 1/d < |k| \approx s\pi/d \ll \Omega$, where $k_1 = \operatorname{Re} k = k_0 - \Delta k_1$, $k_2 = \operatorname{Im} k$, so we have in the main order

$$y'(k_0) = (-1)^S \frac{1}{2} \frac{\Omega d^2}{s\pi}, \quad \bar{y}(k_0) = i(-1)^S \frac{1}{2} \frac{\Omega d}{s\pi}. \tag{4.2}$$

Thus the strong inequalities $|y'(k_0)/d| = |\bar{y}(k_0)| \gg 1$ are satisfied and $\bar{y}(k_0)$ is pure imaginary value when the banding is tight. One may substitute the last expressions into the general formulas of Ref. 1, Appendix A, and Sec. V, and make sure that $|\Delta k_1| \propto s\pi/|\Omega|d$ at zeros and poles of the reflection amplitude, but $k_2 = 0$ at zeros and $|k_2| \propto (s\pi/|\Omega|d)^2$ at poles.

## V. NUMERICAL SIMULATION OF GAUSSIAN WAVE PACKET SCATTERING ON THE LATTICE OF DELTA POTENTIALS

Figures 4–16 show the results of the numerical computation of Gaussian wave packet scattering on the lattice of identical $N = 50$ delta barriers at different values of his spectral characteristics.[12]

Figure 4(a) shows the spectrum of the transmission coefficient $T = T(E)$ of the lattice (2.1) and the spectrum of the group velocities of the free moving of the particle $v_{g0}$ and its moving inside the lattice $v_g$ for the region of energy values covering the second, the third and the fourth transmission bands.
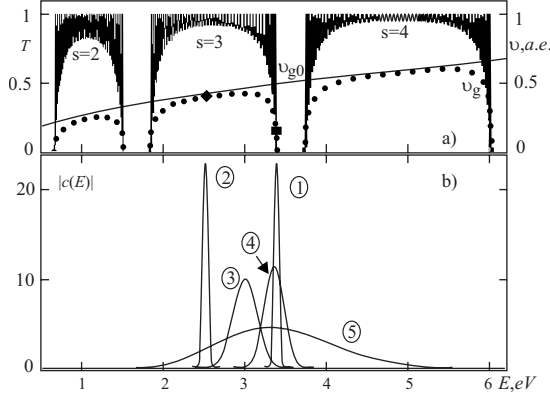
FIG. 4. Scattering of the Gaussian wave packets: (a) the transmission coefficient spectrum $T=T(E)$ for the lattice composed of $N=50$ identical $\delta$ barriers with $\Omega=0.25$ a.u., $d=10$ Å in the region of $s=2,3,4$ transmission bands, and the group velocities of the free moving particle $v_{g0}$ and of the particle moving inside the lattice $v_g$ (black square in the band $s=3$ denotes the value $v_g=0.25$ a.u., measured by the slope of the line 3 in Fig. 11(a), rhomb ($v_g=0.43$ a.u.), by slope of the line 3 in Fig. 11(b); (b) spectral functions $|c(E)|$ for five Gaussian wave packets differing by their energetic position of maximums and by the width of their spectral functions. For the first of them $x_C=-500$ Å, $\Delta x=250$ Å, $E_C=\hbar^2 k_C^2/2m=3.35$ eV, for the second packet the values of $x_C$ and $\Delta x$ are the same as for the first, but $E_C=2.55$ eV, for the third $x_C=-250$ Å, $\Delta x=45$ Å, $E_C=3$ eV, for the fourth $x_C=-250$ Å, $\Delta x=60$ Å, $E_C=3.35$ eV, and for the fifth $x_C=-250$ Å, $\Delta x=10$ Å, $E_C=3.38$ eV.

Figures 5–16 illustrate the results of the numerical computation of the wave functions in the consequent moments of time during the scattering process for five Gauss wave packets differing by their energetic position of maximums and by the width of their spectral functions $|c(E)|$ [Fig. 4(b)], i.e., by their group velocities and space widths.

The quasistationary states in the lattice are excited more effectively if the width $\Delta x$ of the scattering packet is large or approximately equal in comparison with the length of the whole lattice $L \sim Nd$ and the spectral function of packet cover one or few lines of a full resonant transparency near threshold of the transmission band. Figures 5 and 6 show the scattering of such spectrally narrow (coordinately wide) first wave packet from Fig. 4(b), with the spectral maximum lying on the boundary of transmission and attenuation bands covering mainly two upper lines of the full transparency (near the resonant energies $E_{R1} \approx \hbar^2 k_{R01}^2/2m \approx 3378$ eV and $E_{R2} \approx \hbar^2 k_{R02}^2/2m \approx 3362$ eV) in the third transmission band [inset in Fig. 5(a)]. The high energy spectral part of the packet belongs to the attenuation band and is quickly reflected, the low energy spectral components penetrate into the lattice quite slowly, strongly interfering between each other and then pass through the lattice in form of the wave packet with his group velocity be smaller $v_{g0}$. Internal reflection from the boundaries of the lattice is so powerful that during penetration and after the coming out of the transmitted and reflected packets, it leads to the forming of the specific quasistationary state in the lattice: In Fig. 6 it is seen that slowly damping structure with two maximums and with internal swapping of the intensity between them is forming
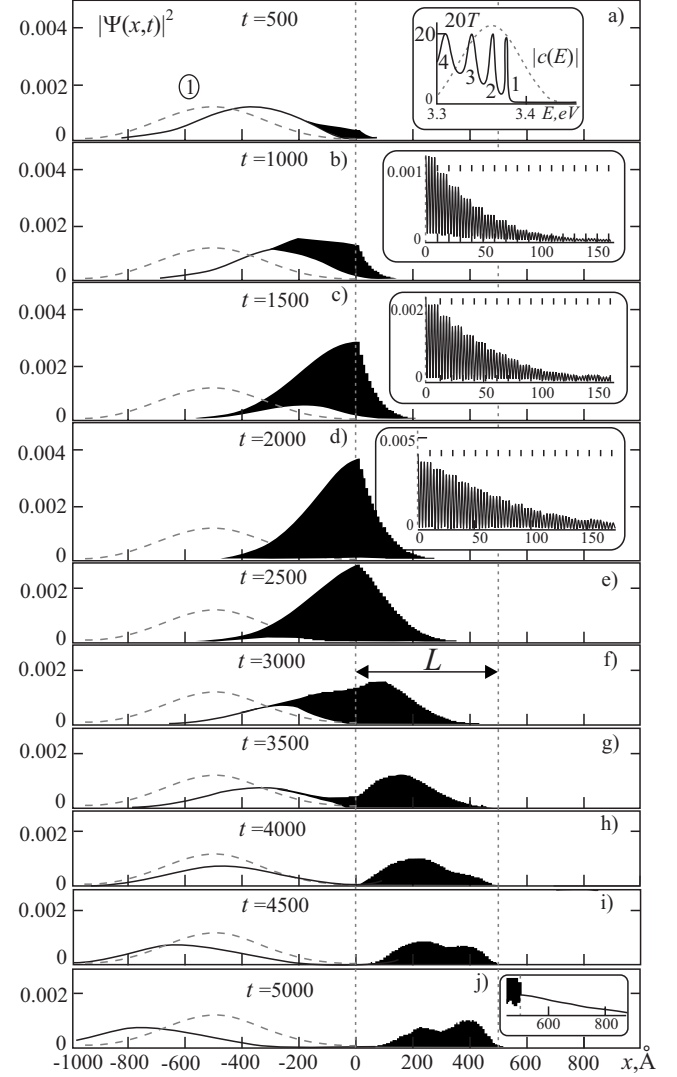
FIG. 5. Initial stages of evolution of the spectrally narrow first wave packet from Fig. 4(b) with the spectral function covering two upper lines of the total transparence [the insertion in (a) sheet] to the transmitted impulse coming out and the quasistationary state forming. The dashed line depicts the initial packet location and dotted line the boundaries of lattice with length $L=Nd=500$ Å; $\delta$ barriers are marked by the touches on the abscissa axis. The insertions show some details of the reflected and transmitted impulses in enlarged scale. The time is measured in atomic units.

inside the lattice after coming out of the reflected and transmitted packets. This structure is described mainly by the superposition of the resonant wave functions from the spectral components with energy corresponding to the mentioned above two upper lines of the full transparency in the third transmission zone, so that the contribution of the utmost of them is small because of its small spectral weight [Fig. 5(a)]. The stationary scattering wave functions of resembling resonance type are shown in Fig. 3 (3,5).

The decay of the quasistationary state leads to the coming out of the secondary wave packets from the lattice to the left and to the right, taking the intensity away (Fig. 6 and Fig. 14).
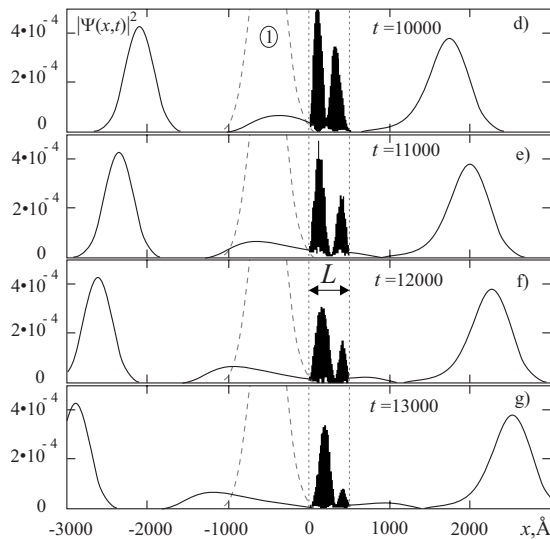
FIG. 6. Next stages of the first packet evolution. The decay of the quasistationary state leads to the coming out of the secondary wave packets following behind the reflected and transmitted impulses.

In Fig. 7 the process of scattering of the similarly spectrally narrow second wave packet accordingly to Fig. 4(b) is shown, it differs from the previous first packet only by the location of its spectral maximum that almost coincide with one of the full transparence lines in the middle of the third transmission zone [inset in Fig. 7(b)]. The values of the transmission coefficient $T(E)$ near this line slightly differ from the unit even in the transmission curve dips. The group velocity of the packet inside the lattice is close to the group velocity of a free moving packet, i.e., the whole packet is almost freely passes though the lattice. Only the small part of it is reflected on the left of the lattice. However, now it is also noticeable the formation of the quasistationary state corresponding to the resonance in the middle of the transmission band (on the stationary state of type 4 from Fig. 3). The decay of this quasistationary state forms outside the lattice the secondary packets are following the reflected to the left [of almost the same intensity Fig. 7(d)] and transmitted to the right [much weaker Fig. 7(e)]. The tails of the coming away secondary packets strongly modulate the resonance quasistationary wave function inside the lattice.

The rest of the wave packets on Fig. 4(b) are "nonresonance." Figure 8 shows the evolution of the third wave packet, with the spectral maximum localized not far away from the middle of the third transmission band and with the spectral function being much wider then the lines of full transparency, but narrower then bandwidth. The transmission of such a packet is large enough, the form and the size of the transmitted packet are the same as the falling packet, the reflected packet is small, and their velocities are equal to $v_{g0}$ [Fig. 11(c)]. While the packet is moving inside the lattice some decreasing of the group velocity and interference modulation of its form take place with the keeping of the form of the envelope. In Fig. 8(e) is the appearance of the weak interferential maximums (the internal reflection) moving to the left near the right end of the lattice.
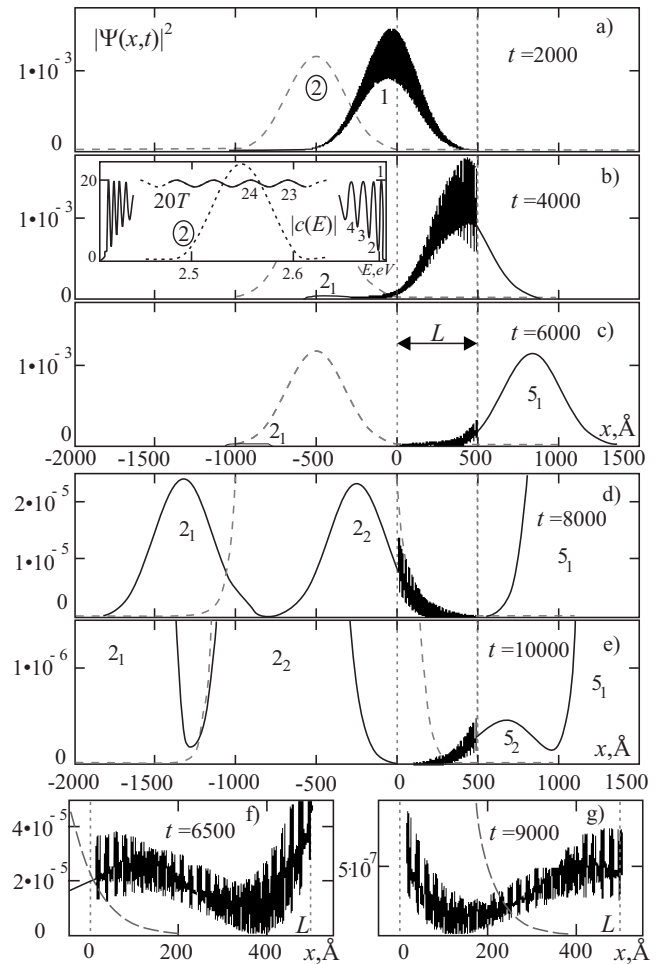


FIG. 7. More complicated behavior and form of the scattering and of the secondary impulses accompanying the scattering of the second packet from Fig. 4(b) with spectral function covering the twenty-fourth line of the total transparency near the middle of the third transmission band [the inset in (b)].

Figure 9 shows the scattering of the fourth wave packet of almost the same width and form as the previous, but with the spectral maximum localized higher by energy (the group velocity of the free moving is higher) on the border of the transmission and attenuation bands. The spectral components falling into the attenuation zone form the powerful reflected packet. The interference of the transmitting and the reflecting components on the borders and inside the lattice is much stronger, the pictured modulus of the wave function has got a specific black color, i.e., the real and imaginary parts of the wave function coherently oscillate by the coordinate with a small wavelength defined by the energy of the packets spectral center $\lambda_C \approx 2\pi/k_C$. After coming out of the main body of the transmitted packet the internal reflection from the right boundary of the lattice and smearing of packets significantly increase. The maximums of impulses move slower inside the lattice than outside of it [Fig. 11(d)].

Figure 10 gives an idea of the scattering of the narrow by the coordinate $x$ but spectrally the most wide by the fifth of the Gaussian wave packets according to Fig. 4(b). Its spectral function by the energetic width covers mainly the third and
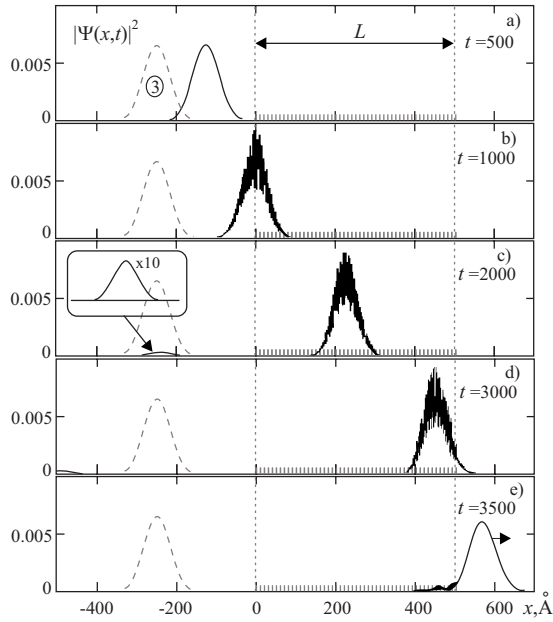
FIG. 8. Evolution of the third wave packet from Fig. 4(b).

the forth transmission bands of the lattice and the attenuation bands lying between and below them. High energy spectral components of the packet covering the forth transmission band form the first rapidly moving to the right and smearing peak $3_1$, spreading initially inside the lattice and then as a leading part of the transmitted impulse. The main part of the packets $3_2$ follows this leader, and it is modulated due to the interference of the spectral components moving with different phase velocities to the right and to the left that belong to the third transmission band. The reflected impulse has two main peaks moving to the left. The first of them that is faster and more powerful is formed by the spectral components covering the gap between the third and the forth transmission bands of the lattice and the second smaller of them is formed
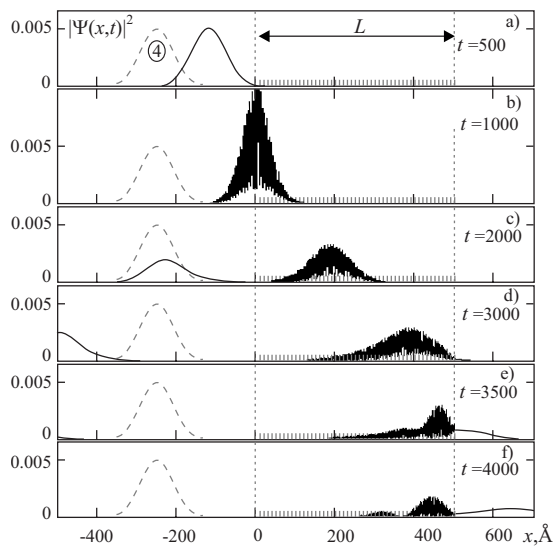


FIG. 9. Evolution of the wave packet with the parameters of the fourth packet from Fig. 4(b).
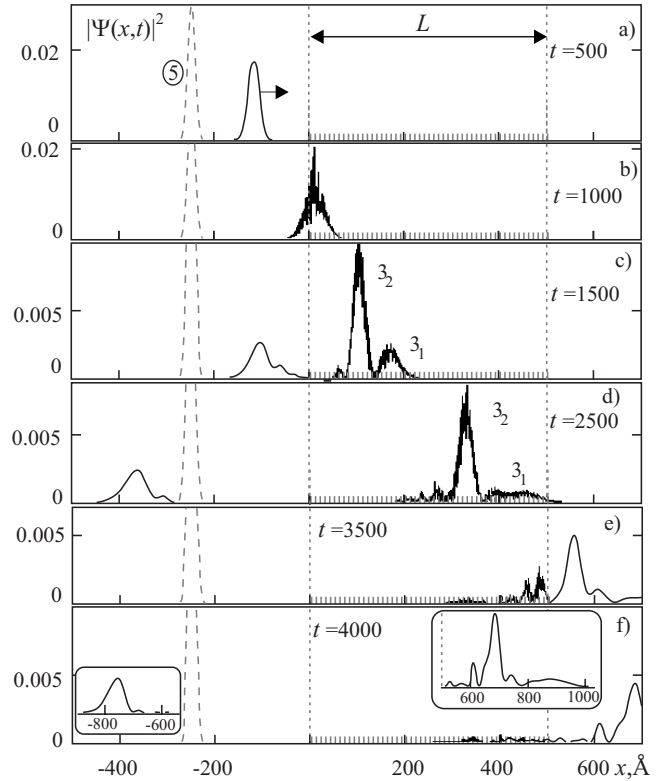


FIG. 10. Evolution of the spectrally wide fifth wave packet from Fig. 4(b) with spectral function covering two transmission bands.

by the slower components covering the gap between the second and the third transmission bands. On the last pictures of the series we can see the long lived tail of the packet near the right end of the lattice.

Figure 11 displays the time dependence of the probability density $|\Psi(x,t)|^2$ with the main peak locations outside and inside of the lattice found from Figs. 5–10. The effects of slowing down of the packets inside the lattice (the diminution of lines slope) and of the delaying of the packets outside the lattice (the shift of the inclined lines) are detectable, so also the formation and decay of the quasistationary states that are generated most effectively by the first and the second packets from Fig. 4(b).

## VI. QUASISTATIONARY STATE

The results of calculation in Figs. 5, 6, 11(a), and 12–16 shows some peculiarities of the formation and decaying of long lived quasistationary states during the transmission of the wave packet through the lattice of finite length.

In Fig. 12 the reflection amplitude $r=r(k)$ zeros and poles in the limits of the third transmission zone are shown. They are calculated for the numerical values of the parameters of the lattice as in Fig. 4(a). In this figure we also show the spectral function $C(k)$ for the first wave packet from Fig. 4(b) and saddle contour of the integration with going around the poles that are closest to the saddle point according to the method of asymptotic calculation described in Ref. 1, Appendix B. It is seen that the poles are located along the pe-
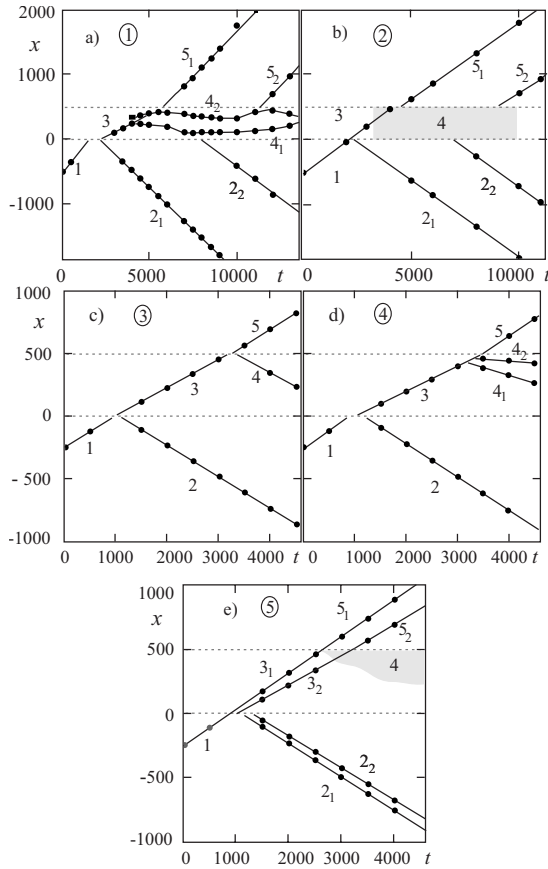
FIG. 11. Points show the coordinates of the main peaks of the nonstationary probability density $|\Psi(x,t)|^2$ plotted against time were evaluated from the numerical computations presented in Figs. 5–10 [the numbers of initial packets by Fig. 4(b) are in ovals], as outside the lattice (1) falling, (2) reflected, and (5) transmitted or generated by the quasistationary states decaying secondary impulses coming out the lattice] so inside the lattice [(3) penetrating, (4) internally reflected or quasistationary] the subscripts enumerate the impulses of the same type following one another. The slopes of lines correspond to the group velocities and their shifts to the delay times. In (a) the lines $4_1$, $4_2$ connected with the existing and $2_2$, $5_2$ with the decaying of the quasistationary states are generated by the first packet, the lines 3 and $4_2$ intersect. Gray strip on (b) locates the region of the quasistationary states are generated by the second packet. Gray strip on (e) locates the tail region of the fifth packet. The variable $x$ is measured in angstroms Å and $t$ in atomic units.

culiar arc in the lower half plane, and the extremes of them are very close to the real axes that results in the long life of the formed quasistationary states. The condition of their formation is a sufficient narrowness and the large value of the spectral function in the area of energy, corresponding to the real part of these poles and zeros related to them.

With the $N$ increasing the number of poles equal to the number of cells is also increasing then the location of poles coming near to the real axes[13] and to the zeros of the reflection amplitude. Figure 13 illustrates the reflection amplitude $r=r(k)$ poles $k_R$ belonging to the third transmission band calculated for the $\delta$ lattices with the same $d$ and $\Omega$ as for Fig. 12, but with the different $N$.
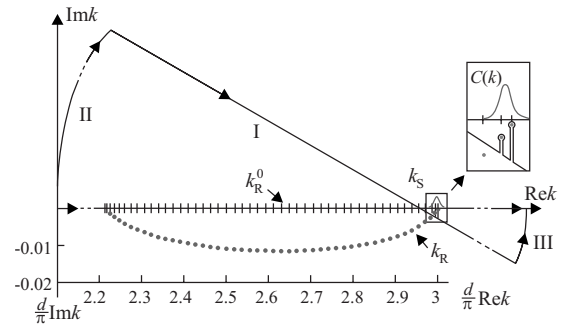


FIG. 12. Poles $k_R$ (points in lower half-plane) and zeros $k_R^0$ (primes on the real axes) of the reflection amplitude $r=r(k)$ in the limits of the third transmission band were calculated for the parameters of lattice and the first wave packet from Fig. 4. The spectral function $C(k)$ and the integration contour with going around the poles that are closest to the saddle $k_S$ are also shown.

In the region $0<x<x_N$ inside the lattice the envelopes of the wave functions $\Psi_{R\nu}(x,t)$ are quite characterized by the values [Ref. 1, (4.7)] of these functions on the nodes

$$\Psi_{R\nu}(nd,t) = -2\pi i \frac{\hbar^2 k_{R\nu}}{m}$$

$$\times e^{-iE(k_{R\nu})t/\hbar} \text{Res}\{c[E(k_{R\nu})]\psi_{0N}[E(k_{R\nu}),x_0+nd]\},$$

where residue is defined by the pole of $r(k)$ from the second term in the expression (3.3) for $\psi_{0N}[E(k_{R\nu}),nd]$, i.e., by the reflected waves. In accordance with Eq. (3.7) this term as a function of $nd$ describes the standing envelope wave $\propto \psi^*(n)$ because of the Chebychev polynomials $U_{n-1}(y)$ are proportional to the $\exp(iKnd)$ and $\exp(-iKnd)$ difference. On the other hand, it is seen from Eq. (3.3) that in the condition of the stationary total transparency when $r(k)=0$ the wave function is $\psi_{0N}(E,x_0+nd)=A_0\psi(n)$. This explains the similarity of the stationary total transparency wave function $\psi_{0N}[E(k_{R\nu}),nd]$ envelope (Fig. 3) and the quasistationary wave function $\Psi_{R\nu}(nd,t)$ envelope inside the lattice (Fig. 6).

The pictures Fig. 5 and 11(a) show that the formation of such a quasistationary states takes place simultaneously with the transmission of the main body $\Psi_S(x,t)$ of the wave packet but these states can exist after the coming out the lattice of the reflected and transmitted nonresonant packets. The nonstationary wave function $\Psi(x,t)$ of developed quasistationary states after the coming out of nonresonant com-
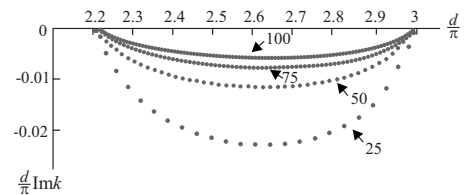


FIG. 13. Poles $k_R$ of the reflection amplitude $r=r(k)$ in the third transmission band were calculated for the same parameters of wave packet as in Fig. 12, but for the $\delta$ lattices with various $N=25$, 50, 75, and 100.
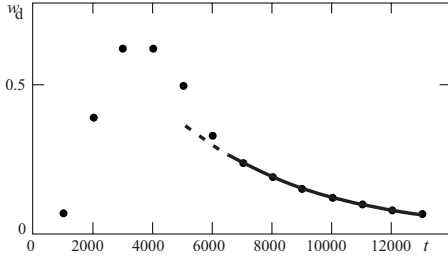
FIG. 14. Points show the probability $w_L$ that was calculated according to the dates of Figs. 5 and 6. The exponential curve is the result of the two parameters fitting by one term from Eq. (6.2) with $\tau_{R2}=4450$ a.u., $t_{02}=550$ a.u., and with $w_{0\nu}=1$. The estimations by [Ref. 1, (4.8)] with coordinates of the second from the right pole on Fig. 12 give $\tau_{R2}=4494$ a.e.; the first from the right pole gives a significantly larger value $\tau_{R1}=16000$ a.u., but its contribution in probability is small on that time interval because of a small spectral weight.

ponents $\Psi_S(x,t)$ near the lattice is approximately equal to the sum of the resonant contributions $\Psi_{R\nu}(x,t)$ that are proportional to residues in the poles lying in the region of spectral function maximum

$$\Psi(x,t) \approx \sum_{\nu} \Psi_{R\nu}(x,t). \qquad (6.1)$$

The probability of the particle detection in quasistationary states inside the lattice is characterized by the integral [Ref. 1, (5.3)] which in the region of exponential decaying is approximately equal to the sum

$$w_L = \int_0^L |\Psi(x,t)|^2 dx \approx \sum_{\nu} w_{0\nu} \exp\left(-\frac{t-t_{0\nu}}{\tau_{R\nu}}\right). \quad (6.2)$$

The numerical calculation of this integral for the first of the investigated wave packets according to the dates of Figs. 5 and 6 gives the points shown in Fig. 14. For the time after the coming out of reflected and transmitted packets [Fig. 11(a)] these points cover well on the exponential curve.

Let us write out the resulting estimations for the lifetime of a quasistationary state for the model of $\delta$ lattice derived by substitution of Eq. (4.2) in the general formulas of the paper in Ref. 1. (a) Near the top of transmission band for the state with number $\nu \ll N$ from [Ref. 1, (5.6)], it follows that

$$\tau_R = \frac{m}{2\hbar}\frac{d}{s\pi}\frac{Nd}{4}\left(\frac{\Omega d}{s\pi}\right)^2\left(\frac{N}{\nu\pi}\right)^2 = \frac{m\Omega^2 d^4 N^3}{8\hbar s^3 \pi^5 \nu^2}, \quad \nu \ll N.$$

Near the bottom of transmission band it is necessary to change $\nu \rightarrow \nu - N$. (b) In the middle of the transmission band from [Ref. 1, (5.7)], we have

$$\tau_R = \frac{m}{2\hbar}\frac{d}{s\pi}\frac{Nd}{4}\left(\frac{\Omega d}{s\pi}\right)^2 = \frac{m\Omega^2 d^4 N}{8\hbar s^3 \pi^3}.$$

For the group velocity $v_g$ and for the time of the transmission through the lattice $\Delta t = Nd/v_g$ of the wave packet main body near the top of the $s$th transmission band from Ref. 1, (5.9) and Ref. 1, (5.10) we get

$$v_g \approx \frac{2\hbar}{m}\frac{(s\pi)^2}{\Omega d^2}\frac{\nu\pi}{N} \approx 2v_{g0}\frac{s\pi}{\Omega d}\frac{\nu\pi}{N} \ll v_{g0},$$

$$\Delta t \approx \frac{m\Omega d^3 N^2}{2\hbar^2 s^2 \pi^3 \nu} = \frac{m}{2\hbar}\frac{d}{s\pi}\frac{\Omega d}{s\pi}\frac{N}{\nu\pi}Nd \approx 4\frac{s\pi}{\Omega d}\frac{\nu\pi}{N}\tau_R \ll \tau_R,$$

where $\nu \ll N$ and $v_{g0}=\hbar k/m \approx \hbar s\pi/md$ is a group velocity of the free moving packet.

In the middle of the $s$th transmission band from Ref. 1, (5.11) and Ref. 1, (5.12) we get

$$v_g \approx \frac{2\hbar}{m}\frac{(s\pi)^2}{\Omega d^2} \approx 2v_{g0}\frac{s\pi}{\Omega d} \ll v_{g0},$$

$$\Delta t \approx \frac{m\Omega d^3 N}{2\hbar^2 s^2 \pi^2} = \frac{m}{2\hbar}\frac{d}{s\pi}\frac{\Omega d}{s\pi}Nd \approx 4\frac{s\pi}{\Omega d}\tau_R \ll \tau_R.$$

That is, at the tight binding conditions a quasistationary state can exist long enough after the passing of the nonresonance parts of the scattered packet.

The almost exponential decay of the quasistationary state is accompanied by the comparatively weak impulses, coming out to the left and right from the lattice, that follow the main transmitted and reflected packets and are well seen in Figs. 6, 7, and 15. They generate the relevant impulses of probability current.

For the first on the Fig. 4(b) wave packet only two terms in the sums (6.1) and (6.2) are significant. The oscillating interference addition to the integral probability $w_L$ is very small due to the approximate orthogonality of the resonance wave functions $\Psi_{R1}$ and $\Psi_{R2}$. But the probability density $|\Psi(x,t)|^2$ includes significant interference terms oscillating in space and in time. The wavelength of coordinate oscillation is $\lambda_b \sim 2\pi/|\Delta k_{12}|$, where $\Delta k_{12}=k_{R01}-k_{R02}$ is the difference of the wave numbers real parts in resonant poles. The period of time oscillation is $T_b \sim 2\pi/\Delta\omega_{12}$, where $\Delta\omega_{12}=(E_{R1}-E_{R2})/\hbar$ is the frequency difference for the main resonance lines are covered by the wave packet. The coordinate oscillations modulate the wave function form inside and outside of the lattice.

Figure 15 shows the coordinate dependence of $|\Psi(x,t)|^2$ at the moment $t=3.5\times10^4$ a.u. $> \tau_{R1} \gg \tau_{R2}$ at the left beyond the reflected packet $2_1$ the interferatively modulated with oscillations $2_2, 2_3, \ldots$ packet follows that is formed by the decay of the quasistationary state. At the right beyond the transmitted nonresonance packet $5_1$ the interferatively modulated with oscillations $5_2, 5_3, \ldots$ packet follows. Inside the lattice [Fig. 15(b)] the envelope of the nonstationary wave function takes a form of the envelope of the first resonance state with higher energy; this wave function has one maximum instead of two maximums as in Fig. 6. This envelope is of the type that is shown in Fig. 3(6).

The time oscillations become apparent brightly in the swinging motion of the $|\Psi(x,t)|^2$ extremums inside the lattice [Fig. 6 and Fig. 11(a)] and in the oscillations of the decay current [Ref. 1, (5.5)]
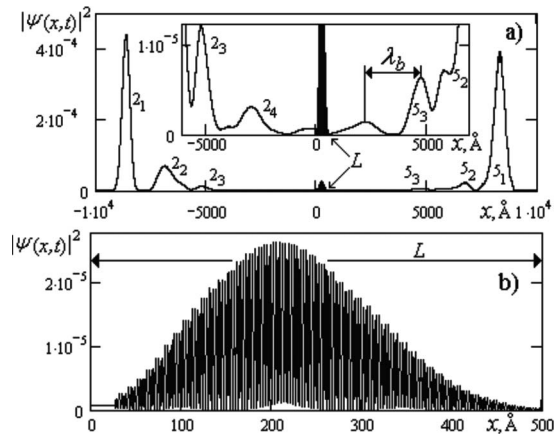
FIG. 15. Probability density after the scattering of the first wave packet from Fig. 4(b) and Fig. 11(a) at the moment $t=3.5 \times 10^4$ a.u. (a) The space oscillations from the beats of two resonance wave functions have the wavelength approximately equal to $\lambda_b \sim 2\pi/|k_{R01}-k_{R02}| \approx 2813$ Å. The inset shows the probability density in enlarged scale. (b) Inside the lattice the wave function took a form of the first resonance state of the type that is shown in Fig. 3(6).

$$j_w \approx \frac{\hbar}{2m}\left[\left(\sum_\nu \Psi_{R\nu}(x,t)\right)\left(\sum_\nu k_{R\nu}\Psi_{R\nu}(x,t)\right)^* + \text{c.c.}\right]$$

(6.3)

in points on the boundaries of the lattice for example. Figure 16 illustrates the probability current that was calculated for the same packet. As it is seen at the point $x=0$ on the left end of the lattice after the positive pulse 1 from the falling packet the negative ones follow $2_1$ from the nonresonance reflected packet and $2_2, 2_3, \ldots$ that are oscillations connected with the beats from the decay of two quasistationary states $E_{R1}$ and $E_{R2}$. At the point $x=Nd$ on the right end of the lattice after the pulse $5_1$ from the nonresonance transmitted packet the oscillations $5_2, 5_3, \ldots$ follow from the decay of the same quasistationary states.
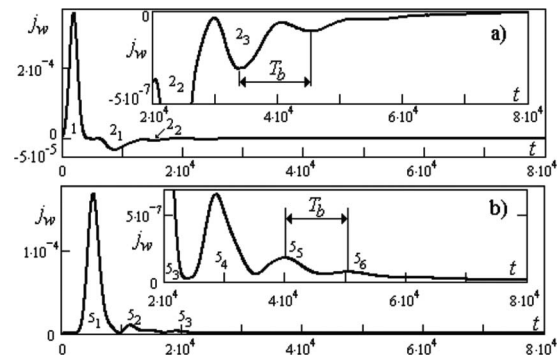


FIG. 16. Probability current for the same packet as in the previous figure: (a) At the point $x=0$ on the left end of the lattice; (b) at the point $x=Nd$ on the right end of the lattice. The inset show probability current in enlarged scale. The period of oscillations is approximately equal to $T_b \approx 2\pi/(E_{R1}-E_{R2}) \approx 10680$ a.e.

These beats will not be observable for the very lengthy packet at $\Delta x \gg Nd$ when the spectral function is narrower than one line of resonant transparency and only one term is large in the previous sums.

## VII. CONCLUSION

The results of numerical experiment by the modeling of the Gaussian wave packet scattering on the finite periodic lattice composed of $\delta$ barriers confirm the theoretical analysis and estimations represented in our paper.[1]

The quasistationary states inside the lattice of $\delta$-barriers are formed by scattering of the wave packet on this lattice after the coming away of transmitted and reflected pulses. The quasistationary wave function envelope is similar to the resonant stationary total transparency wave function envelope and its localization length is approximately equal to the length of the lattice. The lifetimes of these states increase with the lattice length more significantly for the resonance energy near the thresholds of transmission band. The considerable interference effects are observable at the quasistationary states decaying.

[1] Yu. G. Peisakhovich and A. A. Shtygashev, preceding paper, Phys. Rev. B **77**, 075326 (2008).

[2] S. Albeverio, F. Gesztesy, R. Hoegh.Krohn, and H. Holden, *Solvable Models in Quantum Mechanics* (Springer, Berlin, 1988).

[3] A. Ya. Shik, Fiz. Tekh. Poluprovodn. (S.-Peterburg) **26**, 1161 (1992).

[4] *Resonant Tunneling in Semiconductors Physics and Applications*, edited by L. Chang, E. Mendes, and C. Tajedor (Plenum, New York, 1991).

[5] S. L. Konsek and T. P. Pearsall, Phys. Rev. B **67**, 045306 (2003).

[6] S. C. Lee, F. Banit, M. Woerner, and A. Wacker, Phys. Rev. B **73**, 245320 (2006).

[7] V. Petrillo and V. S. Olkhovsky, Cent. Eur. J. Phys. **3**, 339 (2005).

[8] M. Tsuchiya, T. Matsusue, and H. Sakaki, Phys. Rev. Lett. **59**, 2356 (1987).

[9] K. Durinyan, S. Petrosyan, and V. Bellani, Philos. Mag. B **81**, 1201 (2001).

[10] G. Garcia-Calderon and J. Villavicencio, Phys. Rev. A **73**, 062115 (2006).

[11] G. Garcia-Calderon, I. Maldonado, and J. Villavicencio, Phys. Rev. A **76**, 012103 (2007).

[12] The figures have been received by the way of numerical calculation in the condition of a not very tight binding, when the parameter $\Omega/k \sim \Omega d/s\pi \approx 0.5$ (see the captions of Fig. 4 and so on where $\Omega=0.25$ a.e., $d=10$ Å $\approx 20$ a.e., $s=3$). This allowed to make calculation and depict the competitive wave packets in the similar space-time scales.

[13] F. Barra and P. Gaspard, J. Phys. A **32**, 3357 (1999).